Broadband amplification of high power 40 Gb/s channels using multimode Er-Yb doped fiber

Raja Ahmad,[1] Stephane Chatigny[2] and Martin Rochette,[1,*]

[1]*Department of Electrical and Computer Engineering, McGill University, Montreal H3A 2A7, Quebec, Canada*
[2]*Coractive High-Tech Inc., 2700 Jean-Perrin suite 121, Quebec G2C 1S9, Canada*
*martin.rochette@mcgill.ca

Abstract—Broadband amplification of several high power communication channels is demonstrated using a multimode Erbium-Ytterbium doped fiber (EYDF) amplifier. The multimode feature of this amplifier aims at simultaneously enabling wide gain bandwidth and high output power. The amplifier provides a gain bandwidth spanning over the 1535.0 nm-1565.8 nm band. The amplifier also provides a high output power of >30.2 dBm, with ± 2.4 dB natural gain flatness over the bandwidth of interest. The performance of the amplifier is assessed in a 40 Gb/s WDM system, featuring no trace of modal dispersion in the eye diagram and a low power penalty (< 0.4 dB) on the bit error ratio (BER).

OCIS Code: (060.2320) Fiber optics amplifiers and oscillators; (060.2330) Fiber optics communications; (060.4510) Optical communications; (060.2410) Fibers, erbium; (060.2280) Fiber design and fabrication.

References and Links

1. Y. Jaouën, J.-P. Bouzinac, J.-M. P. Delavaux, C. Chabran, and M. Le Flohic, "Generation of four-wave mixing products inside WDM c-band 1 W Er $^{3+}$/Yb^{3+} amplifier," Electron. Lett. **36**(3), 233–235 (2000).
2. J. H. Lee, Z. Yusoff, W. Belardi, M. Ibsen, T. M. Monro, and D. J. Richardson, "A tunable WDM wavelength converter based on cross-phase modulation effects in normal dispersion holey fiber," IEEE Photon. Technol. Lett. **15**(3), 437–439 (2003).
3. Z. Jiao, and X. Zhang, "Experimental Investigation of the Role of Four-Wave Mixing in Supercontinuum Generation From a Multimode 975-nm Pumped Fiber Ring Cavity," IEEE Photon. Technol. Lett. **21**(7), 420–422 (2009).
4. T. Yang, C. Shu, and C. Lin, "Depolarization technique for wavelength conversion using four-wave mixing in a dispersion-flattened photonic crystal fiber," Opt. Express **13**(14), 5409–5415 (2005), http://www.opticsinfobase.org/oe/abstract.cfm?URI=oe-13-14-5409.
5. Y. Deiss, C. McIntosh, G. Williams, and J. Delavaux, "Gain flatness of a 30dBm tandem Er-Er/Yb double-clad fiber amplifier for WDM transmission," in *Optical Fiber Communications Conference*, A. Sawchuk, ed., Vol. 70 of OSA Trends in Optics and Photonics (Optical Society of America, 2002), paper WJ6.
6. A. Sano, Y. Miyamoto, T. Kataoka, and K. Hagimoto, "Long-span repeaterless transmission systems with optical amplifiers using pulse width management," J. Lightwave Technol. **16**(6), 977–985 (1998).
7. M. X. Ma, H. D. Kidorf, K. Rottwitt, F. W. Kerfoot III, and C. R. Davidson, "240-km repeater spacing in a 5280-km WDM system experiment using 8×2.5 Gb/s NRZ transmission," IEEE Photon. Technol. Lett. **10**(6), 893–895 (1998).
8. I. Yoshihisa, "Ultra-long Span Repeaterless Transmission System Technologies," NEC Tech. J. **5**, 51–55 (2010).
9. Y. Miyamoto, A. Hirano, K. Yonenaga, A. Sano, H. Toba, K. Murata, and O. Mitomi, 320 Gbits/s (8x40) Gbits/s WDM transmission over 367-km zero-dispersion-flattened line with 120-km repeater spacing using carrier-suppressed return-to zeron pulse format," in *Optical Amplifiers and their Applications*, S. Kinoshita, J. Livas, and G. van den Hoven, eds., Vol. 30 of Trends in Optics and Photonics (Optical Society of America, 1999), paper SN1.
10. P. Bousselet, M. Bettiati, L. Gasca, M. Goix, F. Boubal, A. Tardy, F. Leplingard, B. Desthieux, and D. Bayart, "dBm output power from an engineered cladding-pumped ytterbium-free EDFA for L-band WDM applications," Electron. Lett. **36**(16), 1397–1399 (2000).
11. G. G. Vienne, J. E. Caplen, Liang Dong, J. D. Minelly, J. Nilsson, and D. N. Payne, "Fabrication and characterization of Yb^{3+}:Er^{3+} phosphosilicate fibers for lasers," J. Lightwave Technol. **16**(11), 1990–2001 (1998).
12. H. Ahmad, S. Shahi, and S. W. Harun, "Bismuth-based erbium-doped fiber as a gain medium for L-band amplification and Brillouin fiber laser," Laser Phys. **20**(3), 716–719 (2010).

13. S. Ohara, N. Sugimoto, K. Ochiai, H. Hayashi, Y. Fukasawa, T. Hirose, T. Nagashima, and M. Reyes, "Ultrawideband amplifiers based on Bi_2O_3-EDFAs," Opt. Fiber Technol. **10**(4), 283–295 (2004).
14. B. O. Guan, H. Y. Tam, S. Y. Liu, P. K. A. Wai, and N. Sugimoto, "Ultrawide-band La-codoped Bi_2O_3-based EDFA for L-band DWDM systems," IEEE Photon. Technol. Lett. **15**(11), 1525–1527 (2003).
15. J. D. Minelly, W. L. Barnes, R. I. Laming, P. R. Morkel, J. E. Townsend, S. G. Grubb, and D. N. Payne, "Diode-array pumping of Er^{3+}/Yb^{3+} Co-doped fiber lasers and amplifiers," IEEE Photon. Technol. Lett. **5**(3), 301–303 (1993).
16. G. G. Vienne, W. S. Brocklesby, R. S. Brown, Z. J. Chen, J. D. Minelly, J. E. Roman, and D. N. Payne, "Role of Aluminum in Ytterbium-Erbium Codoped Phosphoaluminosilicate Optical Fibers," Opt. Fiber Technol. **2**(4), 387–393 (1996).
17. Y. Jeong, J. K. Sahu, D. B. Soh, C. A. Codemard, and J. Nilsson, "High-power tunable single-frequency single-mode erbium:ytterbium codoped large-core fiber master-oscillator power amplifier source," Opt. Lett. **30**(22), 2997–2999 (2005).
18. J. Kringlebotn, J. Archambault, L. Reekie, J. Townsend, G. Vienne, and D. Payne, "Efficient low-noise grating-feedback fiber laser doped with $Er^{3+}:Yb^{3+}$," in *Optical Fiber Communication Conference*, Vol. 4 of 1994 OSA Technical Digest Series (Optical Society of America, 1994), paper TuG5.
19. S. Taccheo, P. Laporta, O. Svelto, and G. De Geronimo, "Theoretical and experimental analysis of intensity noise in a codoped erbium–ytterbium glass laser," Appl. Phys. B **66**(1), 19–26 (1998).
20. V. Philippov, C. Codemard, Y. Jeong, C. Alegria, J. K. Sahu, J. Nilsson, and G. N. Pearson, "High-energy in-fiber pulse amplification for coherent lidar applications," Opt. Lett. **29**(22), 2590–2592 (2004).
21. G. Canat, L. Lombard, A. Dolfi, M. Valla, C. Planchat, B. Augère, P. Bourdon, V. Jolivet, C. Besson, Y. Jaouën, S. Jetschke, S. Unger, J. Kirchhof, E. Gueorguiev, and C. Vitre, "High Brightness 1.5 ̄m Pulsed Fiber Laser for Lidar: From Fibers to Systems," Fiber Integr. Opt. **27**(5), 422–439 (2008).
22. A. Shirakawa, J. Ota, M. Musha, K. Nakagawa, K. Ueda, J. R. Folkenberg, and J. Broeng, "Large-mode-area erbium-ytterbium-doped photonic-crystal fiber amplifier for high-energy femtosecond pulses at 1.55 microm," Opt. Express **13**(4), 1221–1227 (2005), http://www.opticsinfobase.org/abstract.cfm?URI=oe-13-4-1221.
23. G. Nykolak, P. F. Szajowski, J. Jacques, H. M. Presby, G. E. Abate, G. E. Tourgee, and J. J. Auborn, "4×2.5 Gb/s 4.4 km WDM free-space optical link at 1550 nm," in *Optical Fiber Communication Conference, 1999, and the International Conference on Integrated Optics and Optical Fiber Communication*, Vol. Supplement of 1999 OSA Technical Digest Series (Optical Society of America, 1999), paper PD11.
24. J. Ma, M. Li, L. Tan, Y. Zhou, S. Yu, and Q. Ran, "Experimental investigation of radiation effect on erbium-ytterbium co-doped fiber amplifier for space optical communication in low-dose radiation environment," Opt. Express **17**(18), 15571–15577 (2009), http://www.opticsinfobase.org/abstract.cfm?uri=oe-17-18-15571.
25. P. R. Kaczmarek, T. Rogowski, E. Kopczynski, P. Karnas, and K. M. Abramski, "High output power Erbium-Ytterbium doped fibre amplifier," in *Proceedings of International Conference on Transparent Optical Networks, 2008* (ICTON 2008), pp. 350–352.
26. N. Park, P. Wysocki, R. Pedrazzani, S. Grubb, D. DiGiovanni, and K. Walker, "High-power Er-Yb-doped fiber amplifier with multichannel gain flatness within 0.2 dB over 14 nm," IEEE Photon. Technol. Lett. **8**(9), 1148–1150 (1996).
27. E. Desurvire, and J. R. Simpson, "Amplification of spontaneous emission in erbium-doped single-mode fibers," J. Lightwave Technol. **7**(5), 835–845 (1989).
28. J. Koponen, M. Laurila, and M. Hotoleanu, "Inversion behavior in core- and cladding-pumped Yb-doped fiber photodarkening measurements," Appl. Opt. **47**(25), 4522–4528 (2008).
29. C. Simonneau, P. Bousselet, G. Melin, L. Provost, C. Moreau, X. Rejeaunier, A. Le Sauze, L. Gasca, and D. Bayart, "High-power air-clad photonic crystal fiber cladding-pumped EDFA for WDM applications in the C-band," in *Proceedings of European Conference on Optical Communications (ECOC' 2003)*, PH Th4-1-2.
30. M. E. Fermann, "Single-mode excitation of multimode fibers with ultrashort pulses," Opt. Lett. **23**(1), 52–54 (1998).
31. J. P. Koplow, D. A. Kliner, and L. Goldberg, "Single-mode operation of a coiled multimode fiber amplifier," Opt. Lett. **25**(7), 442–444 (2000).
32. J. M. Sousa, and O. G. Okhotnikov, "Multimode Er-doped fiber for single-transverse-mode amplification," Appl. Phys. Lett. **74**(11), 1528–1530 (1999).
33. D. Gloge, "Weakly guiding fibers," Appl. Opt. **10**(10), 2252–2258 (1971).
34. A. D. Yablon, *Optical Fiber Fusion Splicing* (Springer-Verlag, 2005)
35. J. A. Buck, *Fundamentals of Optical Fibers*, 2nd Edition (Wiley, 2004).
36. R.G. Wiley, B.G. Clark, and J. Meitzler, "Compact, active alignment fusion splicer with automatic view-angle compensation," United States Patent. no. 7712981.
37. K. Yelen, L. M. B. Hickey, and M. N. Zervas, "Experimentally verified modeling of erbium-ytterbium co-doped DFB fiber lasers," J. Lightwave Technol. **23**(3), 1380–1392 (2005).
38. G. P. Agrawal, *Lightwave Technology: Telecommunication Systems* (Wiley, 2005).
39. M. Rochette, M. Guy, S. LaRochelle, J. Lauzon, and F. Trepanier, "Gain equalization of EDFA's with Bragg gratings," IEEE Photon. Technol. Lett. **11**(5), 536–538 (1999).

1. Introduction

High-power (>1 W) optical fiber amplifiers, compatible with high data rate channels spreading over the 1530 nm-1565 nm (C-) band spectrum, are of great interest in applications such as nonlinear signal processing [1–4] and optical data transport [1,5–9]. Following the ability of Erbium (Er-) ions to store and emit energy in this wavelength range, the Er-doped fiber (EDF) is a fundamental component of fiber amplifiers. However, conventional EDF amplifiers (EDFAs) have an output power that saturates at a power level $\leq$ 26 dBm [10], even with double-clad fiber geometry, which rules out their use for applications demanding high power. The co-doping of conventional EDFs with rare-earth materials can enhance the pump absorption, which is followed by a non-radiative energy transfer to Er-ions, thereby increasing the maximum output power of the amplifier. Further increase in output power can be realized by using such co-doped fiber amplifiers in tandem with high power multimode pump diodes [11].

While various materials including Bismuth (Bi) can be used as co-dopants for the power scaling of EDFAs [12–14], Ytterbium (Yb)-sensitization of EDFAs is attractive in several ways: (1) It provides amplification over the C-band without significant impairments caused by the nonlinear effects, (2) it helps suppressing the concentration quenching effect, which is the predominant cause of power limitation in conventional EDFAs [15–17,11], (3) it allows shortening the required length of fiber [18] to achieve the same amount of gain as that provided by a conventional EDFA – a consequence of an increased dopant concentration offered by the Yb-sensitized EDFAs – and, (4) it reduces the noise originating from pump power fluctuations [19] by allowing an efficient energy transfer from Yb to Er ions via cross-relaxation process.

Recently, cladding pumped EYDF amplifiers (EYDFAs) have attracted considerable attention to achieve high power levels in line with the requirements of applications like LIDAR [20,21], femtosecond pulse amplification [22], and space communications [23,24]. However, experimental details on the performance evaluation of EYDFAs compatible with WDM signals remain scarce in the literature. To date, the reported gain bandwidth of high power EYDFAs is limited to the 1545-1565 nm band [10,25,26], thereby leaving the available 1530 nm-1545 nm region of the C-band with insufficient gain. A straightforward way to increase the gain in this missing band is to increase the population inversion of Er ions in the EYDF [27]. Taking a cladding-pumped, single mode EYDF as a reference, a successful approach to increase the population inversion is to increase the total pump power that overlaps with the doped area of a given EYDF section [28]. Following this, a first option consists in reducing the cladding diameter while maintaining the same doped core diameter [29]. Although it increases the population inversion, this option is currently impractical because it requires using pump laser with non-standard fiber geometry. A second option which has not been investigated yet, involves increasing the EYDF core diameter while keeping the cladding diameter unchanged. This option allows pumping the double-clad EYDF with commercially available, high power laser diodes, but involves a multimode guidance of the signal. However, preferential seeding [30] and/or bending [31] as well as the optimized fiber parameters [32] can allow for a mainly single-mode operation of multimode fibers.

In this paper, we present a multimode EYDFA that exhibits an extended gain spectrum covering the 1535-1565 nm band with an output power of 30.2 dBm. We choose a multimode EYDF to benefit from a strong and wide gain spectrum without measurable negative impact from the multimode propagation. This is achieved by two mechanisms fostering single-mode propagation. The first mechanism is the mode-field diameter (MFD) of the fundamental mode (LP_{01}) in the EYDF designed to match the MFD of the standard single-mode fibers used to feed and extract the signal in and out of the EYDF. The second mechanism is the gain experienced by the LP_{01} mode in the EYDF which is much stronger than the one for higher order modes [33]. We show that although the EYDF is in fact multimode, the amplified eye-

diagram contains no trace of modal dispersion, as expected from the theoretical analysis. We have also performed the bit error ratio (BER) testing of the EYDFA in a 40 Gb/s WDM system revealing negligible power penalty on the BER.

2. Theory

2.1 Fiber composition

The multimode EYDF, as shown in Fig. 1, is a double-clad fiber with a circular core to guide the signal and an octagonal inner cladding to guide the pump. The core is composed of phosphosilicate glass activated with Er and Yb. The phosphorus content (8-10 mol %) in the core as well as the concentrations of Er and Yb (i.e., 2.6 x 10^{25} ions/m^3 and 4.4 x 10^{26} ions/m^3, respectively) are optimized for an efficient energy transfer while suppressing the unwanted emission from excited Yb-ions. The circular core has a diameter of 10 ¯m and a numerical aperture (NA) of 0.2, which leads to a fiber that is slightly multimode in the C-band, with four LP modes (LP$_{01}$, LP$_{11}$, LP$_{21}$ and LP$_{02}$) allowed to propagate. There is a close match between the fundamental mode of the multimode EYDF and the guided mode of standard G.652 single-mode fibers. Taking advantage of this, patch cords of G.652 are spliced directly at the input and output of the EYDF using a commercially available, optical fiber fusion splicer (Fujikura, FSM-40S). The splicer allows a manual core alignment, which is guided by maximizing the coupled power observed with a power meter. The inner cladding of the EYDF is made of pure silica with an octagonal diameter of 125 ¯m. The numerical aperture of the inner cladding is 0.46, allowing compatibility with commercially available, high-power multimode pumps.
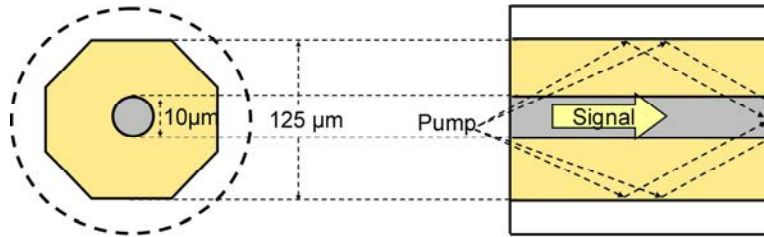

Fig. 1. Geometry of the EYDF.

2.2 Calculation of modal gain

Although the multimode EYDF allows four guided signal modes, only the fundamental mode (LP$_{01}$) significantly benefits of the available gain when the EYDF is fusion spliced to a G.652 single-mode fiber [34]. For an EYDF delivering 30 dBm of output power with a total gain of 15 dB (– in line with the experimental conditions, discussed later in Section 4), the level of amplification of each propagating mode is quantified by taking into account the two processes of higher order mode stripping. The first process arises from the selective mode coupling between the G.652 single-mode fiber and the multimode EYDF that is acting at the input and output of the EYDF. The amount of power transferred from the G.652 fiber to a given LP mode of the EYDF and vice versa, depends on the overlap integral η_{lp} given as

$$\eta_{lp} = \frac{\left| \int_S E_{G.652} E_{lp}^* dS \right|^2}{\int_S \left| E_{G.652} \right|^2 dS \int_S \left| E_{lp} \right|^2 dS}, \tag{1}$$

where $E_{G.652}$ is the transverse mode profile of the fundamental mode in the G.652 fiber, E_{lp} is the transverse mode profile of an LP mode in the EYDF, and S denotes the transverse surface area. The value of the overlap integral for higher order modes of EYDF is much smaller than

that for the fundamental mode (LP$_{01}$), which matches closely with the fundamental mode of the G.652 fiber.

The second process of higher order mode stripping arises from an increased gain coefficient of the EYDF fundamental mode with respect to the higher order modes due its higher confinement into the EYDF gain medium. The confinement factor of a mode (Γ_{lp}) in the EYDF core is the ratio of its power confined in the doped core (P_{core}) to the total power that propagates in the mode (P_{total}) [35],

$$\Gamma_{lp} = \frac{P_{core}}{P_{total}} = \frac{\int_{core} E_{lp} E_{lp}^* dS}{\int_{\infty} E_{lp} E_{lp}^* dS}. \tag{2}$$

Once combined, the two processes of higher order mode stripping provide the net gain of an EYDF-LP mode as $G_{lp} = \eta_{lp}.e^{(\Gamma_{lp} \cdot g \cdot L)}$, where g is the gain per unit length and L (= 2.15 m) is the length of the EYDF.

Table 1. Overlap integral, confinement factor and net gain for each mode of the multimode EYDFA, providing a total gain of 15 dB

	LP$_{01}$	LP$_{02}$	LP$_{21}$	LP$_{11}$
Overlap integral η_{lp}	0.99	4.84 x 10^{-2}	0	0
Confinement factor, Γ_{lp}	0.95	0.27	0.64	0.85
Net gain G_{lp} [dB]	13.56	−19.25	-∞	-∞

Table 1 summarizes the values of η_{lp}, Γ_{lp}, and G$_{lp}$ for each available mode in the EYDF. We note that the LP$_{11}$ and LP$_{21}$ modes are odd modes and thus their overlap integral with the LP$_{01}$ mode of the G.652 fiber is zero. This prevents the coupling of power to LP$_{11}$ and LP$_{21}$ modes, of course, provided the fibers are well aligned which can be ensured to a large extent by employing the commercially available splicing machines. Slight core misalignments are considered in the next section. Calculating the values of overlap integral and confinement factor for the other surviving modes, we find that the fundamental LP$_{01}$ mode in the EYDF, theoretically experiences ~33 dB more gain than the LP$_{02}$ mode. In this way, all the higher order modes are well-suppressed in the fiber, with only the fundamental mode carrying substantial amount of power. No trace of modal dispersion in the eye diagram of amplified signal (discussed further in subsection 4.3) is an experimental proof of higher order modes' suppression.

2.3 Effect of finite cleave angle and core offset

In practice, a minimum splice loss of 0.1 dB between the guided mode of a single mode fiber and the fundamental mode of a multimode fiber like the EYDF, must be ensured to avoid significant excitation of higher order modes [34]. Splicing machines are available with lateral alignment accuracy within a small fraction of core diameter (± 0.1 µm) and an angular alignment accuracy of < 0.1° (see Ref. 36). Figure 2 shows the dependence of coupling loss between the single mode fiber's guided mode and the fundamental mode of EYDF on the alignment of the two fibers during the fusion splicing process [34]. We note that the coupling loss remains sufficiently low for a considerably wide range of lateral as well as angular misalignments. This shows that most of the power from the single-mode fiber is coupled to the fundamental mode of EYDF.
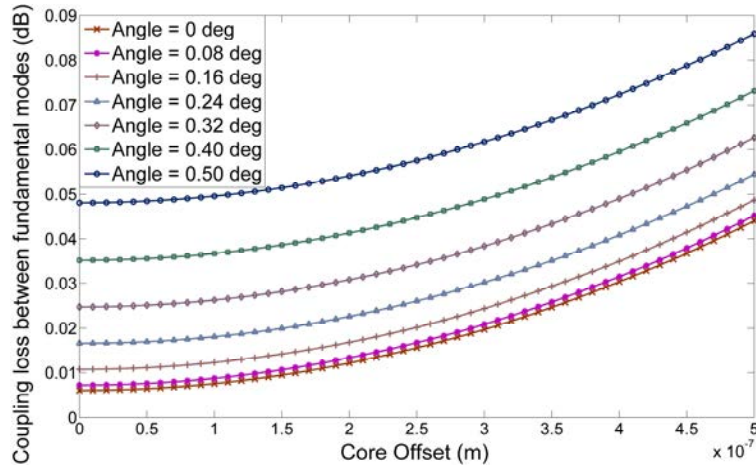
Fig. 2. Bit Coupling loss between guided mode of single-mode fiber and the fundamental mode of EYDF versus the lateral misalignment in terms of core offset for different angular misalignment values.

In short, the EYDF essentially operates as a single-mode fiber for the C-band signal and as a multimode fiber for the 975-nm pump. This reduces the pump depletion in the gain medium (EYDF), which leads to an increased population inversion throughout the fiber and hence, a broadened gain spectrum with respect to a single-mode EYDF. The process of population inversion increase in a multimode EYDF with respect to its single-mode counterpart is discussed below in a more quantitative manner.

2.4 The origin of population inversion enhancement

The population inversion enhancement provided by the multimode EYDF is explained from the theory of gain media. The pump absorption coefficient is approximated as $\alpha_p \approx \frac{1}{2}\left(N^{Yb}\sigma_{p,a}^{Yb} + N^{Er}\sigma_{p,a}^{Er}\right)\Gamma_p$ [37], where N^{Yb} and N^{Er} stand for the ion concentrations; while $\sigma_{p,a}^{Yb}$ and $\sigma_{p,a}^{Er}$ stand for the pump absorption cross sections, of Yb and Er respectively, and Γ_p is the confinement factor of the pump power in the doped core. In the present case, the α_p can be further simplified to $\alpha_p \approx \frac{1}{2}N^{Yb}\sigma_{p,a}^{Yb}\Gamma_p$, owing to the larger absorption cross section of Yb than Er around the pump wavelength and the high Yb/Er concentration ratio, $N^{Yb} \approx 17N^{Er}$. Also, the signal absorption coefficient is given as $\alpha_s \approx \frac{1}{2}N^{Er}\sigma_{p,a}^{Er}\Gamma_s$ [37]. For the pump, Γ_p and hence the α_p increases with the square of the fiber core diameter due to the pump power being uniformly distributed within the octagonal pump waveguide. On the other hand, Table 1 shows that the signal power in the EYDF is mainly concentrated in the fundamental mode owing to its larger values of overlap integral and confinement factor with respect to those for the higher order modes. As a result, the α_s mainly depends on the fundamental mode power confined in the EYDF core. Making the EYDF multimode by increasing the core diameter from 5.9 µm (with V = 2.405) to 10.0 µm results theoretically in a 284% increase in α_p, as opposed to a 6.9% increase in α_s. The relatively large increase in pump absorption than the signal absorption reduces the depletion of pump, which leads to an increased population inversion in the multimode EYDF relative to that in a single-mode EYDF. This increased population inversion in the multimode EYDF is responsible for the broadening of gain spectrum with respect to a single-mode EYDF, by providing gain at the shorter wavelengths of the C-band [27].

3. Fiber structure and length optimization

3.1 Amplifier schematic

Figure 3 shows a schematic structure of the EYDFA. The pump light from a multimode 3.3 W broad-area laser at 975 nm is coupled in counter-propagation to the EYDF via a 2 + 1→1 multimode pump/single mode signal combiner with only one pump input being used. The isolator (ISO 1) installed at the input side of the EYDF eliminates backward amplified spontaneous emission (ASE), whereas the isolator (ISO 2) at the output side blocks outside back-reflections.
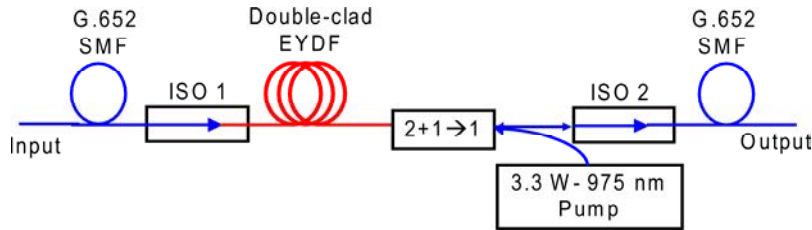
Fig. 3. Schematic of the EYDFA. ISO: Isolator, SMF: Single Mode Fiber.

3.2 Optimization of the EYDF length

The length of EYDF in the amplifier is optimized based on a standard cutback analysis, with an aim to maximize slope efficiency and gain flatness over the spectral range of 1535-1565 nm. For this purpose, we use a WDM signal carrying 11.8 dBm of power and covering the 1535-1565 nm band. Figure 4 shows the total output power versus launched pump power at different fiber lengths between 1 m and 3 m. The slope efficiency with a 1 m-long fiber is lower than with longer fibers as a consequence of incomplete pump absorption. As the length of fiber is increased, the slope efficiency increases before reaching a maximum value of ~34% for a 2.15 m long fiber. From this optimal length, a further increase in fiber length leads to a reduction in slope efficiency. Figure 4 (inset) shows the gain excursion versus the output power for different lengths of the multimode EYDF over the 1535-1565 nm band. We deduce that the 2.15 m long EYDF is optimum for the amplification of high power, broadband signal − since it provides the highest amount of output power with the lowest gain excursion and a reasonably high slope efficiency.
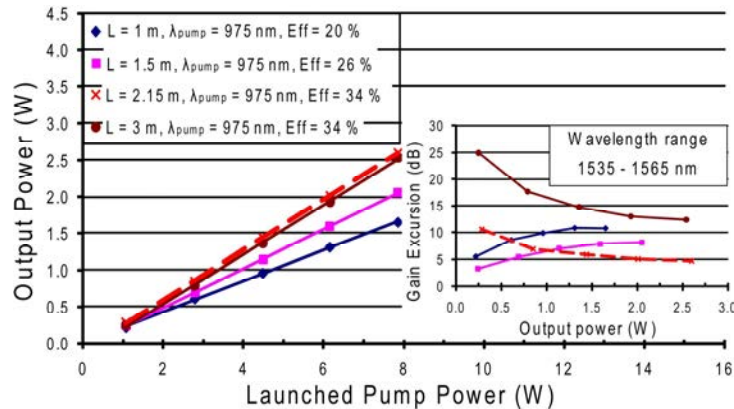

Fig. 4. Total output power versus launched pump power for different lengths of EYDF. Inset: Gain excursion over the wavelength range of 1535-1565 nm versus the total output power.

3.3 Multimode versus single-mode design

To show the advantage of a multimode design over a single mode design, a cutback analysis is also performed on a single-mode EYDF prepared with dopant compositions identical to the multimode EYDF. The single-mode fiber has a core diameter of 7 ¯m. Figure 5 shows the gain spectra for different lengths of the single-mode EYDF as well as the gain spectrum for the 2.15 m long multimode EYDF as a reference. The total output power in each case is approximately 33.9 dBm in response to a WDM input signal of 11.8 dBm. Note that the gain at shorter wavelengths increases as the fiber length is being reduced, but it still remains lower than the gain provided by an equivalent length of multimode fiber which allows an equal amount of pump absorption. The better gain of the multimode EYDF at the short wavelengths arises from an increased population inversion [27] with respect to the single-mode EYDF, as discussed previously in Section 2. Figure 5 (inset) also compares the overall gain excursion over the 1535-1565 nm band, for the corresponding lengths of the two fibers. Note that the multimode fiber provides a lower gain excursion with respect to any of the single-mode fibers.
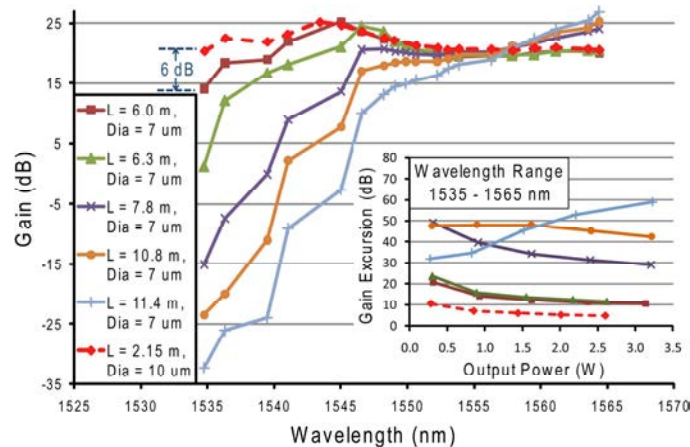

Fig. 5. Gain spectrum for different lengths of single-mode EYDF (core diameter = 7 ¯m) and for 2.15 m of multimode EYDF delivering a total output power of ~33.9 dBm. Inset: Gain excursion over the wavelength range of 1535-1565 nm versus the total output power.

4. High data-rate characterization

4.1 Experimental setup

Figure 6 shows the experimental setup used to characterize and test the optimized EYDFA constructed from a 2.15 m long multimode EYDF – in terms of gain, noise figure (NF), eye-diagram and BER in a 40 Gb/s WDM system. The EYDFA was used in tandem with a pre-amplifier. The use of a low-noise preamplifier and a high-power amplifier (EYDFA) in tandem is greatly beneficial in reducing the overall NF of the amplifying system since the NF of the preamplifier dominates in such a system [38]. A WDM signal consisting of 8 channels spreading from 1530.3 nm to 1564.8 nm was used to measure the gain and noise-figure of the EYDFA by using an optical spectrum analyzer (Agilent-86142B). A tunable probe laser with a power level of −10.2 dBm was used to measure the gain and NF at intermediate wavelengths between the saturating tones, in steps of ~0.4 nm. A BER measurement was performed at 40 Gb/s to measure signal degradation caused by the multimode EYDF in the communication link. The probe channel was modulated in a return to zero (RZ) format with 50% duty cycle, following a pseudo-random binary sequence of length 2^{15}-1. In order to study any signal degradation caused by the EYDFA, the eye diagram of the probe channel was compared on an oscilloscope (Agilent-86100C) with and without the EYDFA in the setup.
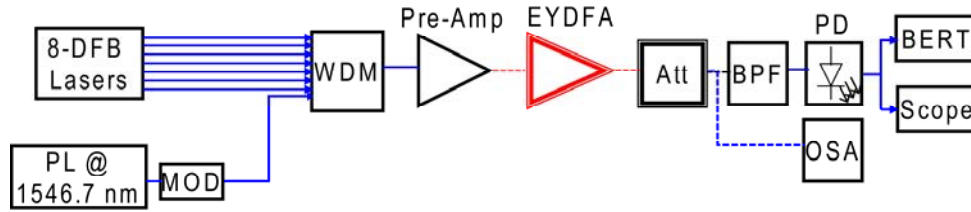
Fig. 6. Gain, NF and Bit error ratio measurement setup. PL: Probe Laser, Mod: Modulator, WDM: Wavelength Division Multiplexer, Att: variable Attenuator, BPF: Bandpass filter @ 1546.7 nm, PD: Photodiode, OSA: Optical Spectrum Analyzer, BERT: BER Tester.

4.2 Gain and noise figure characterization

Figure 7 shows the spectrum of the WDM signal before and after the EYDFA. The WDM signal was spectrally equalized to ± 0.4 dB at the output of the pre-amplifier and totalized 15.9 dBm. The total output power after the amplification was 30.2 dBm for a pump power of 3.3 W. The output power could easily be increased to 34.3 dBm by pumping the EYDFA with 6 W of power.
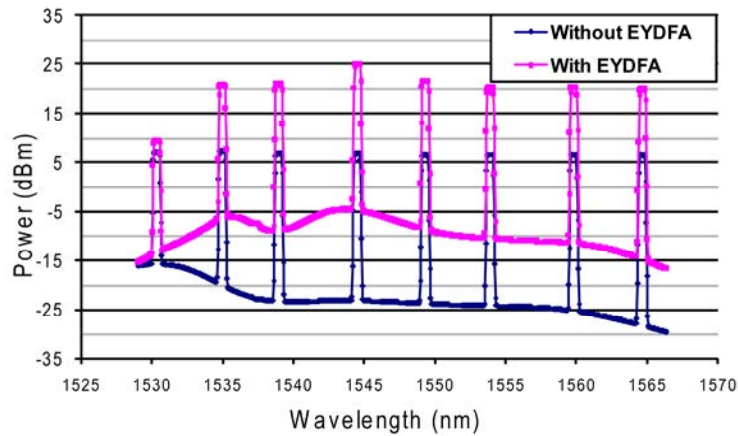

Fig. 7. Spectra before and after amplification of 8 channels spreading from 1530.3 nm to 1564.8 nm.

Figure 8 shows the gain and NF of the EYDFA alone as well as that of the dual-stage amplifier. With a total power of 5 dBm at the input of the preamplifier, the natural gain of the EYDFA reaches a value of 18.4 dB with ± 2.4 dB in flatness over a useful spectral range of 1535.0 nm-1565.8 nm. The gain could be flattened even further by using an appropriate filter in the mid-stage of the dual-stage amplifier [39]. The NF of the EYDFA varies between 4.1 dB and 9.7 dB over the spectral range of interest. The most important noise contribution in the EYDFA arises from the amplified spontaneous emission, filling the available modes of the EYDF and partially coupled to the output fiber. Figure 8 shows that the overall gain of dual-stage amplifier increases as the power at the input of preamplifier is reduced. However, this gain increase is also accompanied by an increase in gain excursion, with the gain spectrum tilting in favor of the channels at shorter wavelengths. It is also observed that the NF of the dual-stage amplifier approaches that of the preamplifier alone as the power at the input is reduced, as expected from theory [38].
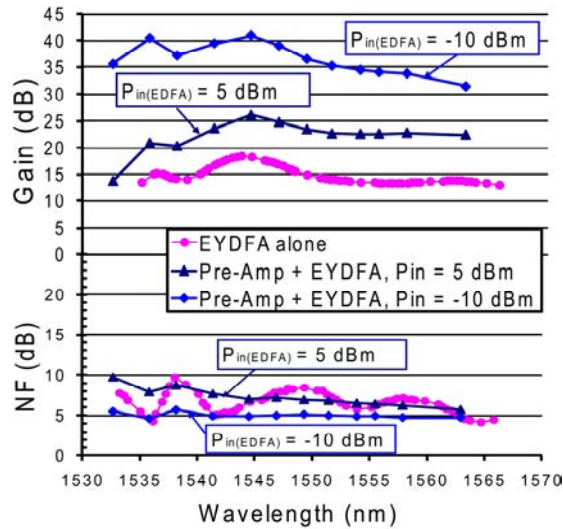
Fig. 8. Gain and noise-figure (NF) of the EYDFA as well as that of the pre-amplifier followed by the EYDFA at different amounts of power at the input of the preamplifier

4.3 Results of BER measurement and eye diagram

Figure 9 shows the BER measurement curves for the 1546.7 nm channel (with NF = 6.9 dB – the average NF of EYDFA over the 1535.0-1565.8 nm band), with and without the EYDFA in the amplifying chain. The result shows that the power penalty leading from the EYDFA is < 0.4 dB. Also, the eye diagram in Fig. 9 (inset) shows no sign of pulse broadening and/or signal distortion. The small amount of power penalty and the unaltered eye diagram, without any sign of modal dispersion shows the negligible degradation of 40 Gb/s WDM signal caused by the multimode EYDFA. This was expected from the theoretical discussion in Section 2.
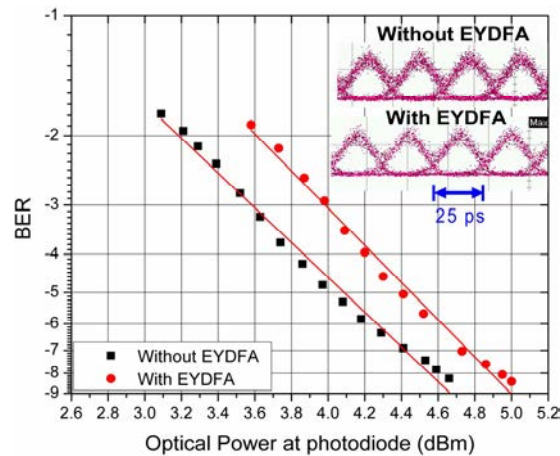

Fig. 9. Bit error ratio and eye diagrams at 40 Gb/s with and without the EYDFA in the communication link.

5. Conclusion

We designed, constructed and characterized a multimode EYDF amplifier which enables the amplification of multiple channels over an extended wavelength span from 1535.0 nm to 1565.8 nm. The wide gain bandwidth of the EYDFA is based on an improved population

inversion of Er-ions in the EYDF leading from a multimode core design. The amplifier provides an output power of more than 30.2 dBm with a natural gain flatness of ± 2.4 dB over the spectral bandwidth of interest. BER measurements in a 40 Gb/s WDM system reveal a negligible power penalty (<0.4 dB) due to the EYDFA. Multimode EYDFAs with large gain bandwidth and high output power can thus be used for signal amplification as needed in the areas of nonlinear signal processing and optical data transport.

Acknowledgment